JCSE The Journal of Corrosion Science and Engineering
ISSN 1466-8858 Volume 16, Preprint 70 submitted 9 December 2013

Effect of hydroxyapatite Sol-Gel coating on corrosion characteristics of titanium alloy implant

Hamid Hessam, hhamid2@live.utm.my

Seyed Morteza Ghaffari Shahri, (Correspondent author) mgsseyed2@live.utm.my

Shahin Hamtaie Pour Shairazifard, hpsshahin2@live.utm.my

Izman bin Sudin, izman@utm.my

Mahtab Assadian, amahtab2@live.utm.my

Address: Departments of Materials, Manufacturing and Industrial Engineering- Faculty of Mechanical Engineering- University Technology of Malaysia (UTM) - UTM 81310, Skudai, Johor Bahru- Malaysia

Affiliation:
Department of Materials, Manufacturing and Industrial Engineering
Universiti Teknologi Malaysia

JCSE The Journal of Corrosion Science and Engineering
ISSN 1466-8858 Volume 16, Preprint 70 submitted 9 December 2013

Abstract

In this study, Dip-coating method is used to coat calcium hydroxyapatite on the Ti-Zr-Nb alloy substrate for orthopaedic applications. Being required to perform sintering process on the coating and acknowledging its impact on the coating bonding and properties, three sintering temperatures with different time spans were used to investigate their effect on the corrosion performance and microstructure of the coating layer. To study the influence of the coating parameters on its performance, immersion and electrochemical corrosion tests were conducted in simulated body fluid. For the purpose of precision, FESEM, XRD and EDS analysis were occupied to characterise the samples before and after aforementioned corrosion evaluation. FESEM characterisation of coated specimens displayed the process at the 600 °C for 10 minutes provides the best corrosion performance, confirmed by observing its consistency. Moreover, immersion in Simulated Body Fluid proved that coating with Hydroxyapatite increases bioactivity resulted from precipitation of calcium phosphate compositions on the coat according to the elements concentration change in the corresponding specimen immersion environment. To do justice to the importance of this research it must be mentioned that dip-coating of hydroxyapatite improves both corrosion performance and bioactivity.

Keywords

Sol-Gel, Hydroxyapatite, Titanium, Corrosion, Microstructure

JCSE The Journal of Corrosion Science and Engineering
ISSN 1466-8858 Volume 16, Preprint 70 submitted 9 December 2013

1. Introduction

Bone injuries and failures attract more and more attention to the field of the implants inception and biomaterials requirements. A vast variety of artificial bone materials, including polymers, metals, ceramics and composites, are discovered to substitute diseased bones [1]. For instance, Cobalt-based alloys (e.g. Co-Cr-Mo), Stainless Steel 316L, Titanium (Ti) and its alloys (e.g. Ti-Zr-Nb) are metallic materials that are commonly employed in place of orthopaedic and dental implants. Ti and some of its alloys could be considered as load-bearing implants thanks to their excellent strength-to-weight ratio and acceptable fracture toughness, supported by superior biocompatibility and high corrosion resistance [2]. Therefore, compared to many metallic materials, the human tissue well accepts Titanium-based family of implants [3]. Furthermore, biological behaviour researches confirm that Zirconium (Zr), being a metal with strong glass-forming capability, could as well guarantee acceptable biocompatibility with a promising non-toxicity. High-volume amorphous Zr-containing structure displays high fracture toughness, high mechanical strength, and high corrosion resistance [4].

Titanium alloys are susceptible to corrosion being used for biomedical applications. However, the corrosion rate of Titanium alloys is low due to oxide layer formation on the surface, forming a protective layer. Alloying and human body aggressiveness, in terms of the corroding environment, result in different types of corrosion which jeopardize the totality of implant properties [5]. Both immersion and electrochemical corrosion tests are applicable to coated samples to determine corrosion rate and mechanisms [6-8].

Hydroxyapatite (HA) [$Ca_{10}(PO_4)_6(OH)_2$] is a favoured coating because of its structural, chemical and biological similarity to human bones and its ability in direct bonding to surrounding tissues [9, 10]. In order to make a combination of HA bioactivity and a titanium alloy mechanical

ISSN 1466-8858 Volume 16, Preprint 70 submitted 9 December 2013

properties, a coating method, which makes the titanium alloy substrates protected against corrosion in the biological environment, is exerted. Additionally, the coating can be used as a barrier against the toxic metal ions being released from substrates to the living body [11]. There are several methods of coating HA namely, thermal spraying [12], magnetron sputtering [13], pulsed laser deposition [14] and sol–gel dip coating [15]. By comparing the mentioned methods, it reveals that sol–gel method owns advantages (low cost, homogeneity, easy to process and doping several ions) which are convincingly enough to conduct the current study by aforesaid method.

Usually, various surface modification techniques are applied to generate ideal characteristics on the surface of different materials. Heat treatment process is considered as an important phase affecting features of sol-gel coating. The aforementioned activity is put to work to reduce cracks appearing on the surface of coated layer. Usually temperature and also time of the heat treatment has a great effect on the coated layer surface [16]. It appears very important to consider smooth surface roughness of coating in order to have a uniform implant-tissue interface. The current study investigates on the effect of Heat treatment parameters on Ti-Zr-Nb alloy coating performance by using three different temperatures and also two different times.

2. Materials and Method

2.1. Material and sample preparation

Ti-Zr-Nb substrates of 2 mm thickness and 5 mm diameter were cut from an as-received rod of a biomedical Ti-Zr-Nb alloy (ASTM F1713-96) and polished by SiC sand-paper (grit 180), and then ultrasonically cleaned in acetone for 10 min, then it kept on rinsing with distilled water 2 times before coating. Table 1 displays the main elemental composition of samples.

ISSN 1466-8858 Volume 16, Preprint 70 submitted 9 December 2013

Substrates were dipped into the sol with speed of 2 cm/min; the coated substrates were dried at room temperature for one day. Then, the coated specimens were sintered for 10 and 30 min at 500, 600 and 700 °C. The coating process was repeated 2 times for the required coatings thickness of 1.5μm.

Table 1. Chemical composition of the alloy used as substrate.

Ti	Nb	Zr	Fe	C	N, H, O	Others
72.3	14.2	13.3	<0.1	<0.1	<0.03	<0.1

2.2. Coating sol

Aqueous solutions of $Na_3PO_4.12H_2O$ and $CaCl_2.2H_2O$ were added to double distilled H_2O. To control the PH at 10.5, NaOH was added to the PO_4 precursor. Next, the PO_4 precursor was added and mixed with the Ca precursor to produce HA.

$10CaCl_2.2H_2O + 6Na_3PO_4.12H_2O + 2NaOH \rightarrow Ca_{10}(PO_4)_6(OH)_2 + 20NaCl + 92H_2O$.

The aforementioned precipitation reaction happens instantly under stirring. The solution was then centrifuged for 5 min at 4000 rpm for 4 times to remove NaCl and H_2O from the resulted emulation. By adding distilled water to the remained solid material at the end of the centrifuge tube and mixing it, it was ensured that NaCl was efficiently extracted from the emulation. At the last time of centrifuging, double distilled water was added to the solid remaining solid material at the end of tube with ratio of $0.1cm^3/g$, and the mixture was agitated prior to coating.

2.3. Characterisation

After pre-treatment (gold coating), the Field Emission Scanning Electron Microscopy (FESEM) instrument utilized was a SUPRA 35VP for analysing the surface morphology of substrates. Energy Dispersive X-ray analyses equip this machine.

JCSE The Journal of Corrosion Science and Engineering
ISSN 1466-8858 Volume 16, Preprint 70 submitted 9 December 2013

2.4. Corrosion test

Electrochemical and immersion tests were performed in simulated body fluid (SBF). The SBF used in this research, which was prepared at 37±0.5 °C, was composed of 8.045 g/l NaCl, 0.355 g/l $NaHcO_3$, 0.225 g/l KCl, 0.231 g/l $K_2HPO_4.3H_2O$, 0.311 g/l $MgCl_2.6H_2O$, 39 ml 1M-HCl, 0.292 g/l $CaCl_2$, 0.072 g/l Na_2SO_4, and TRIS (added by degrees until the desired pH, here 7.4, was achieved).

2.4.1. Electrochemical test

The electrochemical test of the coated samples was performed using a potentiodynamic corrosion test machine (Parstat-2263) and according to ASTM Standard G-5. Graphite and saturated calomel electrode (SCE) were set as counter- and reference electrodes, respectively, with Scanning rate was adjusted to 0.9mV/s. SBF with PH value of 7.4, at 37ºC by using a hot plate, was employed as corrosive media. To prepare the working electrode, the substrates were clamped and mounted, according to figure 1, to insulate it from the media apart from the testing face.

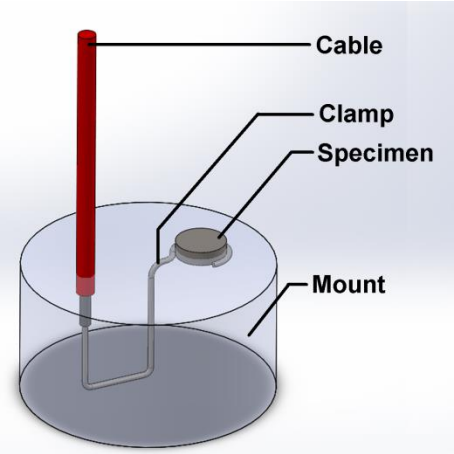

Figure 1. Sketch of mounted specimen for electrochemical test.

2.4.2. Immersion test

ISSN 1466-8858 Volume 16, Preprint 70 submitted 9 December 2013

The ratio of the surface to solution volume was kept constant at 1 cm^2 / 20 ml for all of the immersion tests. The immersion test was performed at 37^oC by keeping the solution in incubator. The substrates of coated and uncoated were immersed for 14 days. Immersed samples surface were analysed by FESEM to evaluate degradation phenomena.

3.0. Results and Discussion

3.1 Surface Morphology Analysis

Surface morphology of HA coating sintered in two different time spans and three different sintering temperatures are shown in figure 2. HA coating on Ti-Zr-Nb sintered at 500ºC showed a porous structure at figure 2.a and 2.b while increasing sintering temperature from 500 to 600 ºC displayed a denser coating layer to be obtained according to Figure 2.c and 2.d. On one hand, increasing the temperature changes the structure of the coating; consequently the appearance of the coating differs due to the growth in different directions, resulting in variation of coating surface integrity. On the other hand, rise in the sintering temperature from 600 to 700 ºC caused cracks, which is exhibited in figure 2.e and 2.f, to be appeared due to thermal contraction difference resulted from higher contraction coefficient of HA (specimens thermal expansion coefficient is 77% of the HA coating layer [17]). The cracks could lead to decrease in mechanical properties of the coating layer as they show existence of residual tensile stress at the interface of the coating and substrate. Moreover, they could be the spots that the coat failure originates. High sintering temperature may result in reducing of biocompatibility of the coating thanks to decomposition of HA structure. Although sintering temperature appeared to be effective on coating morphology, sintering time span variation displayed no significant aftermath. It was concluded that heat treatment at 600^oC for 10 min provides a crack free surface and dense structure. The EDS analysis of HA coating on Ti-Zr-Nb sintered at 600ºC and 10 min

JCSE The Journal of Corrosion Science and Engineering
ISSN 1466-8858 Volume 16, Preprint 70 submitted 9 December 2013

is displayed in figure 3 and is an evidence of carbon contamination, remained from precursor or solvent, on the coating.

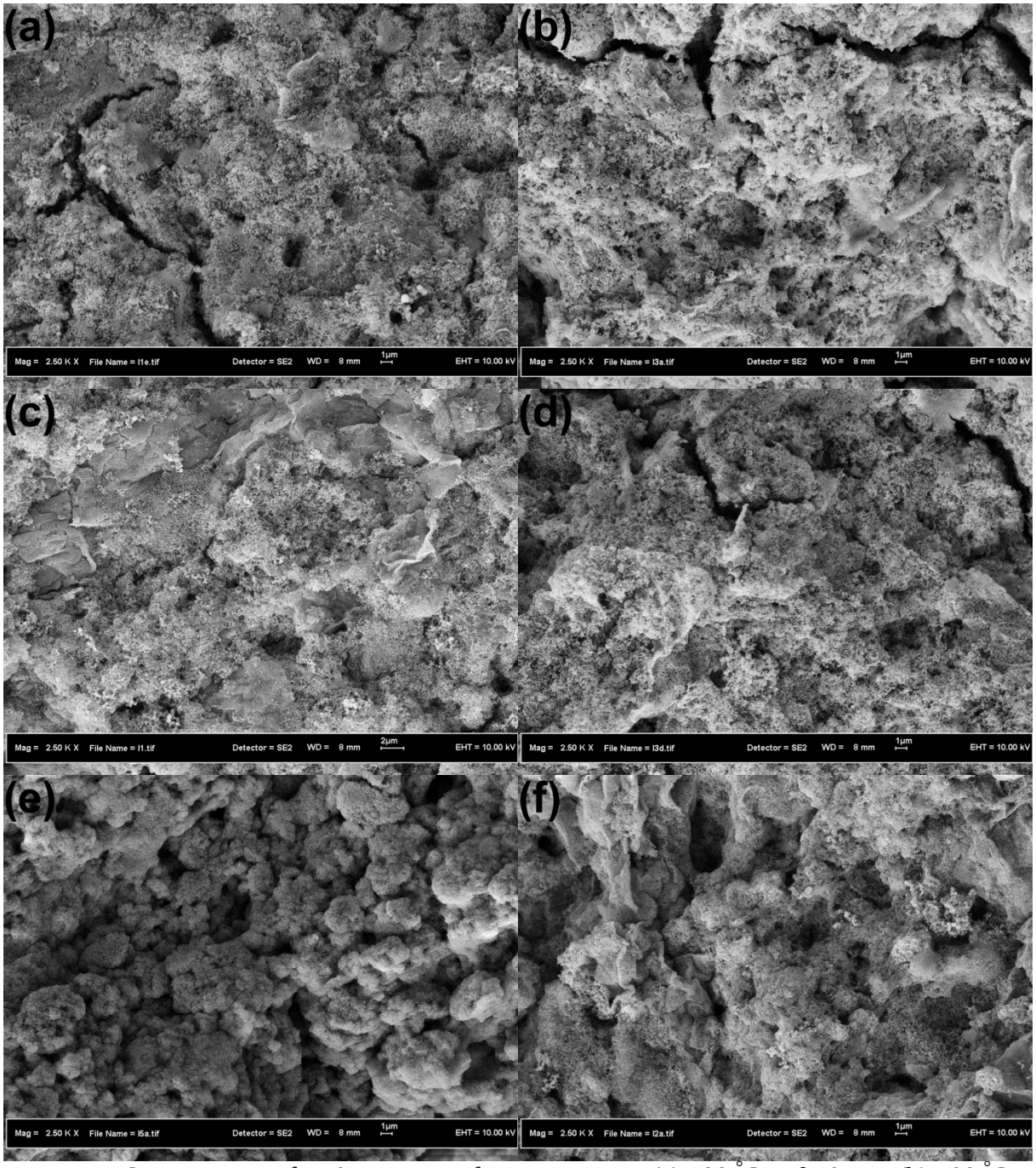

Figure 2. FESEM image of HA coating after sintering at, (a) 500 °C and 10min, (b) 500 °C and 30 min, (c) 600 °C and 10 min, (d) 600 °C and 30 min, (e) 700 °C and 10 min, (f) 700 °C and 30 min

JCSE The Journal of Corrosion Science and Engineering
ISSN 1466-8858 Volume 16, Preprint 70 submitted 9 December 2013

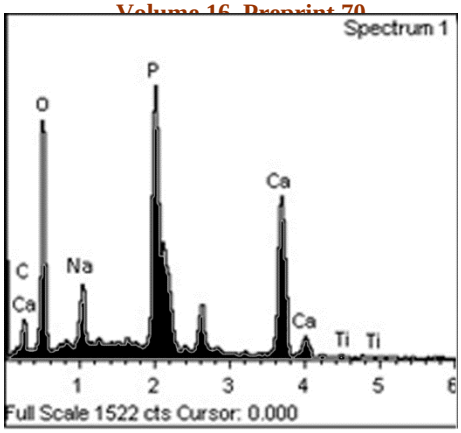

Figure 3. EDS analysis of HA coating over Ti-Zr-Nb sintered at 600ºC and 10 min

Figure 4 illustrates XRD pattern, corresponding to the specimen sintered for 10 min and at 600°C. XRD pattern reveals presence of beta tri-calcium-phosphate β-TCP and CaO due to ion migration from the metallic substrate into the coating layer. A number peaks of HA and TCP phase are observed to be between 20° to 50° of 2θ. The peaks related to the CaO phase are also appeared to be at 30 º, between 40 and 45 º and 55 to 60º of 2θ. The strongest peaks of HA are shown to be at 29º and 31º of 2θ. The reaction and presence of β-TCP and CaO may explain by the following equation:

$Ca_{10}(PO_4)_6(OH)_2 \rightarrow 2\beta\text{-}Ca_3(PO_4)_2 + Ca_3(PO_4)_2{\cdot}CaO + 2H_2O$

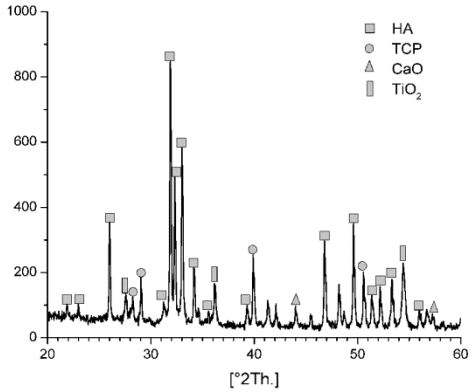

Figure 4. XRD graphs of HA coating on Ti-Zr-Nb for 10 min at 600ºC

JCSE The Journal of Corrosion Science and Engineering
ISSN 1466-8858 Volume 16, Preprint 70 submitted 9 December 2013

Figure 5 shows potentiodynamic patterns of coated sample sintered for 10 minutes at 600°C and a bare sample. The patterns of electrochemical test show lower current density in both cathodic and anodic reactions for the coated sample in comparison with the uncoated sample. The uncoated substrate reveals lower passivation potential and presents a stable passivation. But the coated sample shows shifting to passivity-activity transition. The low slop of cathodic and anodic reaction for the uncoated sample leads to indistinct corrosion rate difference between the samples, while there is a broad gap between the cathodic and anodic patterns of the samples. It is noticeable that coated sample shows less activity rather than the bare one. Table 2 represents the corrosion current and potential. Uncoated sample shows lower corrosion potential and higher corrosion current.

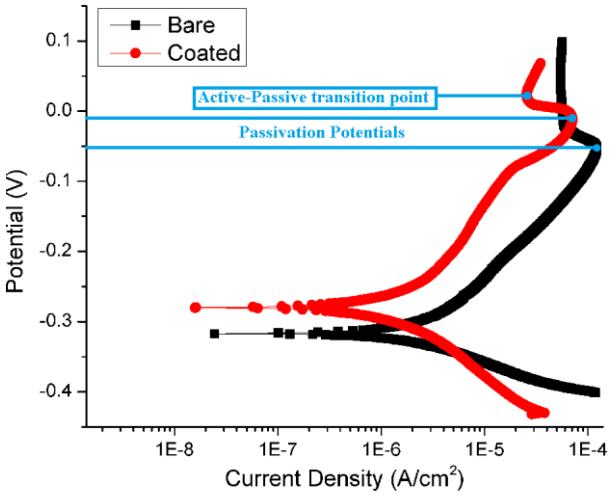

Figure 5. Potentiodynamic patterns of selected coated sample and uncoated sample

Table 2. Corrosion potential and current

	Potential	Current
Bare Sample	-0.32	8×10^{-6}
Coated Sample	-0.27	3×10^{-6}

Immersion

ISSN 1466-8858 Volume 16, Preprint 70 submitted 9 December 2013

According to figure 6.a bare Titanium sample shows localized corrosion phenomena and the presence of corrosion products on the corroded area. The corrosion products are not as dense and uniform as normally observed oxide layers on titanium alloys. The porous formation of the corrosion products leads to preparation of an environment suitable for pitting. Figure 6.b illustrates the surface of HA coated sample immersed for 30 days. Broad cracks are observed in the coat. The cracks are formed when there are valleys near each other. The valleys appearing next to each other are providing weak spots supplied by mechanical stresses from sintering process. The valleys are spots of the coat most near to the sample matrix which owns the highest amount of metallic ions. The metallic ions ignite chemical reactions that stimulate ion transportation from the matrix to the reaction cavity. The ion transportation leads to crack initiation and advance that grows toward another centre of stress in the neighbouring.

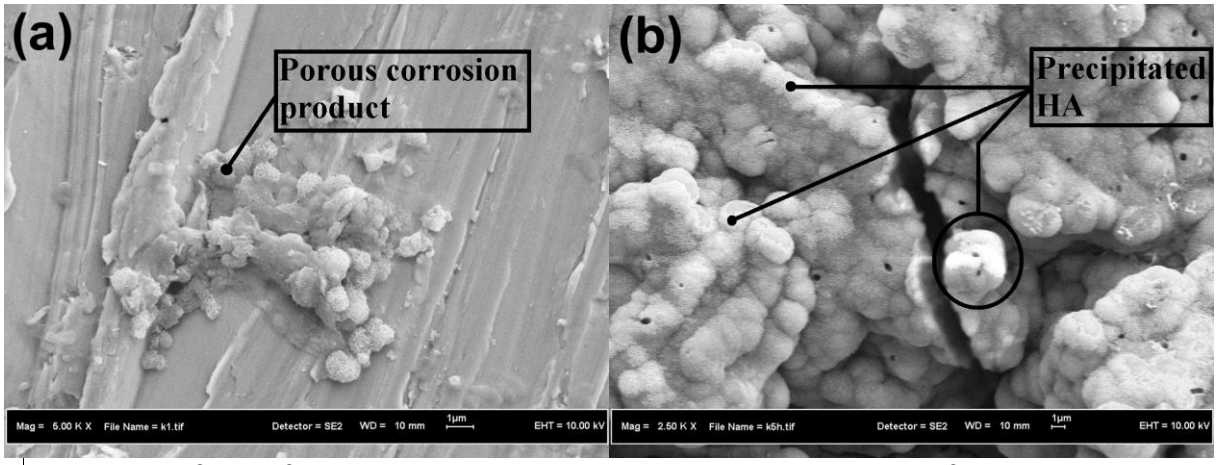

Figure 6. Surfaces of immersed (a) uncoated and (b) HA coated sample for 30 days in SBF.

Figure 7 and figure 8 show calcium and phosphate concentration in the SBF, in which coated and uncoated specimens were soaked, respectively. On one hand, generally, P and Ca concentration in SBF corresponding to coated specimens showed increase as time passed. On the other hand, Ca and P of the SBF corresponding to uncoated specimens showed levelling or negligible

ISSN 1466-8858 Volume 16, Preprint 70 submitted 9 December 2013

decrease. For the SBF corresponding to the coated specimens, HA coat degrades in the solution and causes intensification in the ions concentration. The degradation initiates fast due to all the weak and sharp edges dissolving rapidly resulted from their weak nature. As time passes, the trend of degradation settles down due to smoothening of the coat surface and precipitation of amorphous Ca/P compositions on coat interface with the solution. Decreasing the slop of the graphs related to coated samples shows the initiation of apatite formation on the coating surface. Fast degradation of the coat leads to releasing Ca^{2+} and H^{+} and consequently raises OH^{-} which increases pH. Accumulation of OH^{-} and pH rise is believed to be necessary for apatite precipitation of the coating surface [18]. For the SBF corresponding to uncoated specimens, Ca and P concentration is only subjected by local corrosion phenomenon.

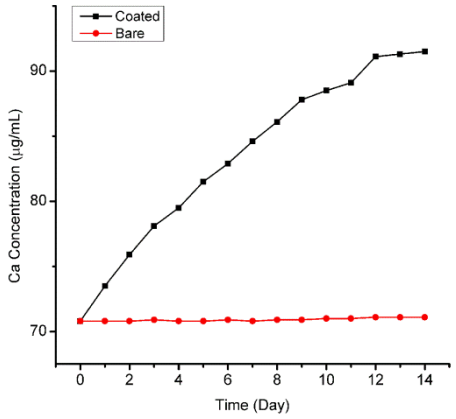

Figure 7. Ca concentration in SBF corresponding to soaked specimens for various time

JCSE The Journal of Corrosion Science and Engineering
ISSN 1466-8858 Volume 16, Preprint 70 submitted 9 December 2013

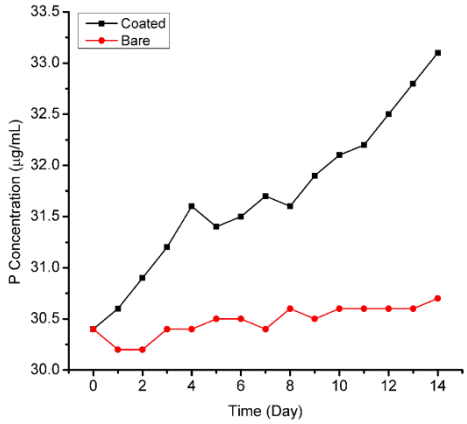

Figure 8. P concentration in SBF corresponding to soaked specimens for various time

4. Conclusions

FESEM observation showed that by increasing of the sintering temperature from 500 ºC to 600 ºC not only the amount of porosity decreased and denser structure obtained but also the best coat integrity of this experiment achieved, whilst, sintered HA coat at 700 ºC with both 10 and 30 min show cracks due to contraction coefficient difference between substrate and coating layer.

XRD patterns show the presence of beta tri-calcium-phosphate (β-TCP) and CaO due to ion migration from the metallic substrates into the coating layer showing coating calcination.

Coated sample lower current and potential in electrochemical corrosion test reveals improvement in corrosion performance. While, immersion test revealed higher bioactivity of the specimens by both changes occurred in surface morphology and Ca and P concentration rise in corresponding specimens' immersion environment.

References

1. 'Evaluation of adhesion strength and toughness of fluoridated hydroxyapatite coatings', Zhang, S., Wang, Y., Zeng, X., Khor, K., Weng, W.Sun, D., *Thin Solid Films*, 516, 16, pp5162-5167, 2008.

ISSN 1466-8858 Volume 16, Preprint 70 submitted 9 December 2013

2. 'Adhesion strength of sol–gel derived fluoridated hydroxyapatite coatings', Zhang, S., Xianting, Z., Yongsheng, W., Kui, C.Wenjian, W., *Surface and Coatings Technology*, 200, 22, pp6350-6354, 2006.
3. 'Surface properties and cell response of fluoridated hydroxyapatite/TiO< sub> 2</sub> coated on Ti substrate', Lee, H., Jeong, Y., Park, S., Jeong, S., Kim, H.Cho, C., *Current Applied Physics*, 9, 2, pp528-533, 2009.
4. 'Hydroxyapatite/titania sol–gel coatings on titanium–zirconium alloy for biomedical applications', Wen, C., Xu, W., Hu, W.Hodgson, P., *Acta biomaterialia*, 3, 3, pp403-410, 2007.
5. 'Ti based biomaterials, the ultimate choice for orthopaedic implants–A review', Geetha, M., Singh, A., Asokamani, R.Gogia, A., *Progress in Materials Science*, 54, 3, pp397-425, 2009.
6. 'Corrosion behaviour and bioactivity of electrophoretically deposited hydroxyapatite on titanium in physiological media (Hanks' solution)', Mohamed, S. G., Abdeltawab, A. A.Shoeib, M. A., *Materials Science-Poland*, 30, 3, pp231-239, 2012.
7. 'Electrochemical behavior of cold sprayed hydroxyapatite/titanium composite in Hanks' solution', Zhou, X.Mohanty, P., *Electrochimica Acta*, 65, 0, pp134-140, 2012.
8. 'Sol- gel- modified titanium with hydroxyapatite thin films and effect on osteoblast- like cell responses', Kim, H. W., Kim, H. E., Salih, V.Knowles, J. C., *Journal of Biomedical Materials Research Part A*, 74, 3, pp294-305, 2005.
9. 'Sol–gel derived fluoridated hydroxyapatite films', Cheng, K., Han, G., Weng, W., Qu, H., Du, P., Shen, G., Yang, J.Ferreira, J., *Materials Research Bulletin*, 38, 1, pp89-97, 2003.
10. 'SOL-GEL DERIVED TITANIA COATING ON TITANIUM SUBSTRATE', LATIFI AFROUZ, A. A., BEHNAM GHADER, A.JOUGHEHDOUST, S., *IRANIAN JOURNAL OF PHARMACEUTICAL SCIENCES*, 2008.
11. 'Surface morphology examination of sol-gel deposited TiO< sub> 2</sub> films', Anast, M., Jamting, Å., Bell, J.Ben-Nissan, B., *Thin Solid Films*, 253, 1, pp303-307, 1994.
12. 'Plasma sprayed hydroxyapatite coatings on titanium substrates Part 1: Mechanical properties and residual stress levels', Tsui, Y., Doyle, C.Clyne, T., *Biomaterials*, 19, 22, pp2015-2029, 1998.
13. 'Microstructure and mechanical properties of hydroxyapatite thin films grown by RF magnetron sputtering', Nelea, V., Morosanu, C., Iliescu, M.Mihailescu, I., *Surface and Coatings Technology*, 173, 2, pp315-322, 2003.
14. 'Pulsed laser deposition of hydroxyapatite thin films on Ti-5Al-2.5 Fe substrates with and without buffer layers', Nelea, V., Ristoscu, C., Chiritescu, C., Ghica, C., Mihailescu, I., Pelletier, H., Mille, P.Cornet, A., *Applied surface science*, 168, 1, pp127-131, 2000.
15. 'Improvement of bonding strength to titanium surface by sol–gel derived hybrid coating of hydroxyapatite and titania by sol–gel process', Im, K.-H., Lee, S.-B., Kim, K.-M.Lee, Y.-K., *Surface and Coatings Technology*, 202, 4, pp1135-1138, 2007.
16. 'Thermal processing of hydroxyapatite for coating production', Gross, K.Berndt, C., *Journal of biomedical materials research*, 39, 4, pp580-587, 1998.

ISSN 1466-8858 Volume 16, Preprint 70 submitted 9 December 2013

17. 'Thermal expansion of hydroxyapatite between − 100 °C and 50 °C', Miyazaki, H., Ushiroda, I., Itomura, D., Hirashita, T., Adachi, N.Ota, T., *Materials Science and Engineering: C*, 29, 4, pp1463-1466, 2009.
18. 'Bone-like apatite formation on HA/316L stainless steel composite surface in simulated body fluid', FAN, X., CHEN, J., ZOU, J.-p., WAN, Q., ZHOU, Z.-c.RUAN, J.-m., *Transactions of Nonferrous Metals Society of China*, 19, 2, pp347-352, 2009.